Terahertz Oscillations in an $In_{0.53}Ga_{0.47}As$ Submicron Planar Gunn Diode

Ata . Khalid,[1,a] G. M. Dunn,[2] , R. F. Macpherson[2], S. Thoms,[1] D. Macintyre,[1] C. Li,[1] M. J. Steer,[1] V. Papageorgiou,[1] I. G. Thayne,[1] M. Kuball,[3] C. H. Oxley,[4] M. Montes Bajo,[3] A. Stephen,[2] J. Glover,[4] and D. R. S. Cumming[1]

[1]*School of Engineering, University of Glasgow,Glasgow,G12 8LT, UK*

[2]*School of Engineering and Physical Sciences, University of Aberdeen, Aberdeen, AB24 SFX, UK*

[3]*H. H. Wills Physics Laboratory, University of Bristol, Tyndall Avenue, BS8 1TL, UK*

[4]*Electronic Engineering Dept., Faculty of Technology, De Montfort University, Leicester, LE1 9BH, UK*

The length of the transit region of a Gunn diode determines the natural frequency at which it operates in fundamental mode – the shorter the device, the higher the frequency of operation. The long-held view on Gunn diode design is that for a functioning device the minimum length of the transit region is about 1.5μm, limiting the devices to fundamental mode operation at frequencies of roughly 60 GHz. Study of these devices by more advanced Monte Carlo techniques that simulate the ballistic transport and electron-phonon interactions that govern device behaviour, offers a new lower bound of 0.5μm, which is already being approached by the experimental evidence that has shown planar and vertical devices exhibiting Gunn operation at 600nm and 700nm, respectively. The paper presents results of the first ever THz submicron planar Gunn diode fabricated in $In_{0.53}Ga_{0.47}As$ on an InP substrate, operating at a fundamental frequency above 300 GHz. Experimentally measured rf power of 28 μW was obtained from a 600 nm long ×120 μm wide device. At this new length, operation in fundamental mode at much higher frequencies becomes possible – the Monte Carlo model used predicts power output at frequencies over 300 GHz.

I. INTRODUCTION:

The Planar Gunn diode is a solid-state rf source consisting of two electrodes, cathode and anode, deposited on the surface of a semiconductor. The electrons entering the semiconductor from the cathode travel through the channel to the anode, under the applied bias. Although discovered more than fifty years ago, the Gunn diode remains an extensively used solid-state source in microwave and mm-wave applications [1-3]. However, the demand for higher frequency applications is growing and a solid-state source for THz frequencies is needed. The received wisdom about Gunn diodes is that, for GaAs the minimum transit region for which a device can be expected to function is well over a micron in length [9-14]. The standard limit quoted for simple vertical devices (essentially one dimensional device) is for a transit region of approximately 1.5 μm and correspondingly a maximum fundamental mode frequency of about 60 GHz [13].

[a] Author to whom correspondence should be addressed. Electronic mail: ata.khalid@glasgow.ac.uk

However, there is increasing evidence that this assumed limit is perhaps not as absolute as previously thought. Experiments with short vertical Gunn diodes have shown operation of vertical Gunn devices with a transit region as short as 0.7 μm [15], and have reported operation of short Gunn diodes at frequencies well in excess of previously theoratical limits [16]. Published work with planar Gunn diodes has demonstrated that operation frequencies of up to 110 GHz are possible [17] in GaAs and at over 160 GHz in $In_{0.53}Ga_{0.47}As$ for 1.3 μm long devices [18]. In recent years, planar Gunn diodes have shown consistent improvements in frequency towards the THz region of electromagnetic spectrum [3]. The first hetero-structure AlGaAs/GaAs based planar Gunn diode operation above 100 GHz was demonstrated in 2007 [19]. Higher frequency of operation is limited by the saturation velocity in GaAs [20]. In order to achieve higher frequencies, a new material system possessing high electron saturation velocity is needed. $In_{0.47}Ga_{0.53}As$ lattice-matched to InP is one possible material system and recently the first $In_{0.47}Ga_{0.53}As$ based planar Gunn diode has shown oscillations at 164 GHz in fundamental mode [18]. So far, the minimum channel length of any planar Gunn diodes reported in the literature has been greater than one micrometer and it is the channel length and saturation electron velocity that determines the oscillation frequency. Semiconductor materials such as, $In_{0.47}Ga_{0.53}As$, InN, InSb GaN and InP have sufficiently large electron velocity, compared to GaAs and are therefore suitable choices [20].

A submicron planar Gunn diode is expected to oscillate at higher frequencies using such semiconductor materials [21]. In recently reported simulation results, a 300 nm long Gunn diode in InN was predicted to reach 0.8 THz [22]. Gunn oscillations have yet to be observed in nitride based systems and there has been no experimental demonstration of a submicron planar Gunn diode operation in several other existing material based systems including InP or InSb. This is in part due to the difficulties of achieving nanometer separation between the anode and cathode with tens of micrometer width. The other possible reason is the main stream research relied upon the theoretical limit that was set longer than micrometer long anode-cathode spacing [13]. Moreover, planar Gunn device technology was ignored in favor of existing vertical Gunn devices that produce higher power at present.

In this paper, a new fabrication process similar to one used for making field effect transistors [23] is presented to realise the first submicron planar Gunn diode using an epitaxial layer of $In_{0.53}Ga_{0.47}As$ on a semi-insulating InP substrate. The measured spectrum show an oscillation at 307GHz. The highest measured power was 28 μW. This is the first ever experimental demonstration of THz oscillations, meeting the expectations of theoretical predictions [22] and that of our own Monte Carlo simulations. These planar Gunn devices are excellent candidates for many applications requiring a solid-state THz source for monolithic integration. The metal cavity encapsulated vertical Gunn diode with mechanical tuning controls, on the other hand, are not suitable for chip integration and portable applications.

II. EXPERIMENTAL

The device fabrication techniques and experimental measurements of the planar Gunn diode are described in the following sub-sections. The fabrication technique for a submicron separation of anode-cathode contact with several tens of micron width is difficult to achieve. There are many reports of submicron field-effect transistors [23-24], however, all nanometer gate field-effect transistors have drain-source separation larger than one micron while sub-micron drain-source separation is achieved using a T-gate shadow. In planar Gunn diodes there is no gate electrode to create a shadow mask for submicron anode-cathode separation; therefore, a new fabrication technique has been developed using two layers of electron beam resist separated by Si_3N_4 to achieve submicron separation for up to 120μm wide anode and cathode contacts.

A. Device Fabrication

InGaAs layers were grown using MBE on a 600 μm thick semi-insulating InP substrate. The active channel layer was 300 nm thick with a doping level of 8×10^{16} cm^{-3}. This was followed by a 200 nm thick cap layer of $In_{0.53}Ga_{0.47}As$ with a doping level of 2×10^{18} cm^{-3}. The cap layer helps to achieve low Ohmic contact resistance to the devices. The channel layers are designed to keep the nL_{ac} product of the devices above 10^{12} cm^{-2} where n is free carrier concentration and L_{ac} is the separation between anode and cathode [25]. For the submicron diode the channel layer thickness was adjusted using wet chemical recess etching during the final step of fabrication. Figure 1 show the device layers and the channel layer thickness adjustment as the dotted line. Substrates were initially spin coated with a 300 nm of PMGI SF6 (supplied by Microchem) and 50 nm of silicon nitride was then applied using a room temperature PECVD process for use as a parting layer. A further 300 nm of UVIII resist (supplied by Chestech ltd) was then applied. A Vistec VB6 UHR EWF large area electron beam lithography tool was used to pattern anode and cathode electrodes with dimensions of 120 μm × 80 μm and various anode-cathode separations down to 100 nm. The UVIII layer was developed for 60s in CD26 at room temperature and washed in DI water. The parting layer was then etched. To create an undercut profile suitable for metal lift off, a low bias oxygen etch process was used to etch back the sacrificial PMGI layer by a controlled amount. The fabrication process was found to be very successful in defining wide anode-cathode structures up to 120 μm with short channels (L_{ac}). Figure 2 shows the main features of the fabrication process used. The rest of the fabrication process is the same as previously reported for the fabrication of 1.3 μm long planar Gunn diodes [18]. Figure 3 shows an SEM image of a completed submicron planar Gunn diode. The inset in the Figure 3 shows a close-up of a 600 nm long channel. The fabricated device yield was over 95% and batch to batch fabrication showed a L_{ac} tolerance of 40 nm.

B. Characterisation

1. DC Measurements

Data is presented only for devices with $L_{ac} \geq 600$ nm owing to the frequency limitation of our test equipment. Pulsed current voltage characteristics of the devices were measured with a semiconductor device analyzer (Agilent Technologies B1500A) using a semi-automated probe station (Cascade Microtech Summit 12K).

Figure 4 shows data from a 600 nm×120 μm device. The pulse width was 500 μs (1 ms pulse period) and the knee of the current occurs at about 0.5 V. The current in the device saturates around 1 V. Above 1 V the current in the device shows a linearly increasing trend. Figure 4 also shows current voltage characteristics of a 1.3 μm long planar Gunn diode plotted for comparison with submicron device. The low bias region clearly shows the lower current levels in a 1.3 μm channel device compared to 600 nm long channel device and it is attributed to longer channel length of the former. The channel current saturates in a submicron device at half the applied bias needed for a 1.3 μm long device.

2. Spectrum Measurements

Since conventional vertical Gunn diodes are constructed in resonant cavities and signal of the oscillators is extracted using rectangular waveguide that has cut-off frequency, therefore multiple constructions operating different frequency bands are required to test the devices and identify the fundamental mode of their oscillations; planar Gunn diodes, on the other hand, are integrated with coplanar waveguides (CPWs) that have no cut-off frequency limitation. This configuration allows device oscillation frequency to be measured for the entire band . Figure 5(a) shows the oscillation identification setup for J-band operation (220 GHz-325 GHz) that consists of a 50 GHz spectrum analyzer (Agilent 4448), a J-band 50 μm GSG probe (GGB Industries), a J-band harmonic mixer (Farran Technology WHM-03) with integrated an LO doubler and an amplifier. A bias-T integrated probe was used to dc-bias the devices. The system insertion loss was approximately 80 dB according to the manufacturer's specifications. This setup allowed accurate identification and location of the oscillation frequency of the devices using the signal identification aid built-in the spectrum analyzer. Lower frequencies were rejected by the J-band waveguide.

Figure 5(b) shows the measured spectrum of a typical device with L_{ac} = 600 nm. Oscillation at 307 GHz is observed. A small downward frequency shift (21.13 MHz), characteristic of Gunn oscillator, was observed as the bias voltage increased from 3.31 V to 3.33 V. This represents a frequency shift rate of 1.06 GHz/V. In order to verify the 307 GHz signal come from a fundamental oscillation of the device rather than a harmonic from a lower frequency oscillation, similar measurements were

carried out at V-band (50 GHz-75 GHz), W-band (75 GHz-110 GHz), D-band (110 GHz-170 GHz) without success in observing any oscillations at other frequencies.

3. RF Power Measurements

Since the conversion loss of the mixer is not accurately specified by the manufacturer, a separate power measurement setup, as schematically illustrated in Figure 6 (a), was used to measure the power level of the signal. The power measurement setup used the same probe as for the spectrum measurement setup but with the mixer, diplexer and spectrum analyzer replaced by a power sensor (Virginia Diode Inc.) and a power meter (Erikson PM4). Since the power senor has a W-band (75 GHz-110 GHz) waveguide input, a J-band-to-W-band taper was used between the probe output and the sensor head input. A W-band right-angle H-bend waveguide was also used between the taper and the power sensor head. The setup has an approximate cut-off frequency of 173 GHz because of the cutoff-frequency of the TE10 mode of the J-band waveguide. This means that no power from oscillation frequencies lower than 173 GHz could be detected. The overall insertion loss from probe to instrument was determined using the manufacturer's data sheets to be 3dB. Figure 6(b) shows the measured power as the applied bias varies from 2.85 V to 3.16 V. A maximum rf power of 28 μW was measured, after de-embedding the 3 dB system insertion loss. The DC current was approximately 63 mA at a voltage of 3.11 V. Since two different measurements techniques were used, a small discrepancy between spectrum measurement (peak signal at 3.31V) and rf-power meter measurements (peak power at 3.11V) was observed. Similar equipment setup was used for the D-band (110 GHz-170 GHz), W-band (75 GHz-110 GHz) and V-band (50 GHz-75 GHz) but no RF power was observed. This evidence proves further that the 307 GHz signal identified by the spectrum analyser as a fundamental oscillation is correct.

III. Monte Carlo Modeling

The simulations carried out were performed using two proprietary Monte Carlo models developed by the authors. Details of these models can be found in previously published papers, for the one-dimensional model in [26] and for the planar model in [27]. The models incorporate acoustic, polar optic and inter-valley scattering processes, use a Poisson solver to recalculate the electric field at femtosecond time intervals and track the behaviour of approximately 20000 super-particles. Mesh size varied depending on the scale of the device under study, naturally, but always lay between a lower bound of 0.5 nm and an upper bound of 1.7 nm. As it is customary for vertical devices, many Gunn diodes incorporate a doping notch to encourage domain formation. The simulation explores the limits of Gunn function and so, while numerous simulations were performed without a notch, it is perhaps unsurprising that these simulations did not produce a functioning device. As a result,

all the vertical Gunn diodes discussed below feature an ideal doping notch. In case of planar Gunn diodes, the doping notch was not used and still produces functioning devices i.e. devices showing Gunn oscillations.

Simulations of GaAs based planar Gunn diodes such as those reported in [28-30] showed a similar natural limit in size with devices shorter than 0.7 µm struggling to operate. Better results were obtained from the InGaAs structure. The domain was observed to be about half of the transit region size (0.6 µm) and this 0.3 µm domain was the smallest observed. This observation is consistent with the predictions of the one-dimensional model. No smaller domain or higher frequency operation was observed in this structure and thus seems to imply a limit. Further work would be required to thoroughly explore the limit. Nevertheless, InGaAs materials have a greater mobility than GaAs and the improved frequency performance is shown in Figure 7 which shows the potential of fundamental mode operation above 300GHz. Figure 7 shows the inverse variation of output frequency with L_{ac} for Monte Carlo simulations [27] and experimental measurement results. In the case of submicron devices, the operation was always found to be in an accumulation mode, not dipole. The accumulation layers formed a little closer to the anode than cathode (about mid way) and grew in size as they transferred from the cathode to anode at the saturation velocity. The resulting frequency was well approximated by $f = 2.25\times10^5/L_{ac}$ Hz (a little over twice the saturation drift velocity of about $0.9\times10^5 ms^{-1}$ in GaAs and $1.1\times10^5 ms^{-1}$ at $1x10^6$ Vm^{-1} in InGaAs [31]) over the distance between anode and cathode L_{ac}) [8,17]. Higher biases were needed in the simulation to maintain accumulation layer oscillations as L_{ac} was decreased. This resulted in significant impact ionization being observed in the simulation and the measured upwards trend in the measured DC characteristics (Figure 4) of the submicron planar Gunn diode confirms this observation. The submicron planar Gunn devices needed to be operated close to breakdown.

In order for a domain to form, not only must the doping transit region length product exceed $10^{12} cm^{-2}$ [32] (as first proposed by Kroemer in 1965 [33]), but there must be the requisite charge density over the domain to contain the required potential and importantly, there must also be the ability for valley populations to change over the width of the domain which will be a function of the inter-valley transition rate. The applied potential must of course be such that the threshold electric field for inter-valley transfer is reached and preferably much exceeded. This potential will depend on the size of the device, doping and domain size, but fields within the domain need to clearly exceed $4x10^5 Vm^{-1}$ in both GaAs and InGaAs [31]. Only when these conditions are met can electrons transition to higher valleys in the conduction band, becoming heavy and slowing, and for electrons ahead of the resulting accumulation of electrons and existing in a region of lower field to have lower effective mass and, concordantly, increased velocity. This allows the domain to form. The minimum size of a domain is therefore a complicated function of the electron velocity, density, electric field and inter-valley scatter rate. As mentioned above, no simulation resulted in a domain smaller than 0.3µm. Generally speaking, the size of a forming domain will be larger than an

established domain. At the start it is known that a forming domain can span the entire transit region in a small device. As its peak moves closer to the anode, the field becomes stronger and the domain reduced in extent. It is reasonable to assert therefore, that whilst the minimum size of an established domain is about 0.3 μm, it needs more room than this to form initially. As a result, the minimum length for the transit region of a functional Gunn operator becomes of the order of 0.5 μm. This new figure is less than one third of the previous limit and results in an operational frequency that is, at over 300 GHz, substantially higher than previously ascribed limits for GaAs Gunn devices and about twice that which has so far been achieved experimentally in the published work. Agreement between theory and experiment is reasonably good, as shown in Figure 7, though the simulations systematically record frequencies about 10% higher than those observed in the real devices at the higher frequencies. This is attributed to the dimensions tolerance of the actual fabricated devices and the simulated device dimentions.

IV. DISCUSSION

Supported by experimental results, the work described in this paper explores the function of Gunn operation at submicron lengths. Simulations using Monte Carlo methods have shown that Gunn diodes may function with transit regions down to 0.5 μm in length. This is substantially smaller than the long-standing expectation that such devices would not work below 1.5 μm. Since the transit region length is intrinsically related to the frequency at which the devices operate, the new submicron devices discussed in this paper allow increases in the frequency of operation. The historically accepted limit for fundamental mode GaAs Gunn diodes of 60 GHz has already been doubled in using planar Gunn devices and this work shows that this frequency can be exceeded by nearly four-fold in InGaAs based planar Gunn diodes. Improvements in modeling techniques have allowed a greater understanding of the electron dynamics within the domain and the complex interplay between electron density, velocity and inter-valley scatter rates that allow domains to form. This has pushed up the theoretical limit of the frequency. Empirically, the achievement of higher doping densities in the planar devices and use of materials with faster inter-valley transition rates have pushed up physically realized frequencies. As the experimental planar Gunn device have a quite highly doped transit region, thermal generation within such a device may be significant, and one area worth further study would be the transport of heat within such devices.

While the Monte Carlo simulations were initially conducted for GaAs, the theory it discusses applies equally well to other NDR materials, including InP and InGaAs, as well as Gallium Nitride (GaN). As relaxation times in these materials are much quicker than in GaAs and mobilities are higher, it may be possible that devices constructed from these materials might operate with still shorter transit regions and consequently higher frequencies for a given transit region length. Simulations of

InGaAs planar diodes have shown the potential for operation at frequencies as high as 350 GHz whilst the experimentally measured devices have shown operation above 300 GHz.

V. CONCLUSION:

In conclusion, the first submicron (600 nm × 120 μm) $In_{0.53}Ga_{0.47}As$/InP planar Gunn diode has been fabricated and found to oscillate above 300 GHz. The highest observed power was 28 μW. It is thought that the oscillations occur in the fundamental mode, based on measurements made across a wide band and simulations carried out using Monte Carlo technique. The fabrication technique lends itself to device arrays to make very high power sources. The proposed $In_{0.53}Ga_{0.47}As$/InP planar Gunn diode with a higher level of output power shows great potential as a solid-state source of terahertz radiation.

ACKNOWLEDGMENTS

This work was supported by UK Engineering and Physical Science Research Council (EPSRC) and e2v Technologies (UK) Ltd. All devices were made with the help of staff in the James Watt Nanofabrication Centre at the University of Glasgow.

REFERENCES

1. J. B. Gunn, "Microwave oscillation of current in III-V semiconductors," *Solid State Commun.*,vol. 88, no.11-12, pp. 883-886, Dec. 1963.
2. K. Sekido, M. Takeuchi, F. Hasegawa, and S. Kikuchi, "CW oscillations in GaAs planar-type bulk diodes," *Proc. of the IEEE*, vol. 57, no.5, pp. 815-816, May 1969.
3. D. L. Woolard, E. R. Brown, M. Pepper, and M. Kemp, "Terahertz frequency sensing and imaging: a time of reckoning future applications?" *Proc. IEEE*, vol. 93, no. 10, pp. 1722–1743, Oct. 2005
4. Förster, A, Stock, J, Montanari, S, Lepsa, M I, Luth, H, Fabrication and characterisation of GaAs Gunn diode chips for applications at 77 GHz in automotive industry, Sensors 6 4 (2006), pp 350 – 360.
5. Bott, I B, Fawcett W, The Gunn Effect in GaAs, Advances in Microwaves, 3 (1968), p 223.
6. Fank, B, Crowley J, Hang, C, InP Gunn Diode Sources, Proceedings of SPIE – The International Society for Optical Engineering, 544 (1985), pp22-28.
7. Kroemer, H, Negative conductance in semiconductors, Spectrum, IEEE, vol.5, no.1 (1968), pp.47-56.
8. Bosch, B G, Engelmann, R W H (1975). Gunn-effect Electronics. New York: Pitman Publishing.
9. Thim, H W, Turner, J. (1993). Microwave Sources. In: Moss, T S, Hilsum, C Handbook on Semiconductors. Amsterdam: Elsevier Science Publishers. p503.
10. Bosch, R, Thim, H W, Computer simulation of transferred electron devices using the displaced Maxwellian approach, IEEE Transactions on Electron Devices, 21, no.1, pp. 16- 25, Jan 1974.

11. Rolland, P A, Friscourt, M R, Dalle, C, Lippens, D, Comparison between InP and other semiconductor, materials for the realization of millimeter wave two terminal devices, Indium Phosphide and Related Materials, 1990. Second International Conference. , vol., no., pp.80-83, 23-25 Apr 1990.

12. Torkhov, N A, Bozhkov, V G, Kozlova, A V, Samoilov, V I, Modified operating regime of gallium arsenide Gunn diodes with thin base, Microwave and Telecommunication Technology (CriMiCo), 2010 20th International Crimean Conference, pp181-182, 13-17 Sept. 2010.

13. Prokhorov, E D, Dyadchenko, A V, Mishnyov, A A, Polyansky, N E, Low power consumption MM-band GaAs oscillators, 2005 15th International Crimean Conference Microwave and Telecommunication Technology, 1 (2005), 1564854, pp 168-169.

14. Hobson, G S. (1974). The transferred-electron effect and space-charge instabilities. In: The Gunn Effect. Oxford: Clarendon Press. pp3-20.

15. Amir, F, PhD Thesis, School of Electrical and Electronic Engineering, The University of Manchester (2011).

16. Amir, F, Mitchell, C, Farrington, N, Missous, M, *Advanced Gunn diode as high power terahertz source for a millimetre wave high power multiplier*, SPIE Europe Security + Defence (Berlin 2009).

17. Pilgrim, N J, Khalid, A, Dunn, G M, Cumming, D R S, Gunn Oscillations in Planar Heterostructure Devices, Semicond. Sci. Technol. 23 (2008) 075013.

18. A. Khalid, C. Li, V. Papageogiou, G. M. Dunn, M. J. Steer, I. G. Thayne, M. Kuball, C. H. Oxley, M. M. Bajo, A. Stephen, J. Glover, and D. R. S. Cumming, "$In_{0.53}Ga_{0.47}As$ planar Gunn diodes operating at a fundamental frequency of 164 GHz" *IEEE Electron Device Lett.*, vol. 34, no. 1, pp. 39-41, Jan. 2013.

19. A. Khalid, N. J. Pilgrim, G. M. Dunn, M. C. Holland, C. R. Stanley, I. G. Thayne, and D. R. S. Cumming, "A planar Gunn diode operating above 100 GHz," *IEEE Electron Device Lett*., vol. 28, no. 7, pp. 849-851, Oct. 2007.

20. M. V. Fischetti, "Monte Carlo simulation of transport in technologically significant semiconductors of the diamond and zinc-blende structures. II. Submicrometer MOSFET's," *IEEE Transactions on Elec. Dev.*, vol. 38, no. 3, pp.650-660, Mar. 1991.

21. S. Perez, T. González, D. Pardo, and J. Mateos, "Terahertz Gunn-like oscillations in InGaAs/InAlAs planar diode," *J. Appl. Phys.*, vol.103, no.9, pp.4516-4518, May 2008.

22. L. Yang, S. Long, X. Guo, and Y, Hao, "A comparative investigation on sub-micrometer InN and GaN Gunn diodes working at terahertz frequency," *J. Appl. Phys.* Vol.111, no.10, pp.4514-4518, May 2012.

23. S.Thoms and D.S.Macintyre, "Long nanoscale gaps on III-V substrates by electron beam lithography,"*J.Vac. Sci. Technol, B* vol.30, no.6, pp. 06F305-06F305-7, Nov. 2012.

24. G. Moschetti, P. Nilsson, A. Hallen, L. Desplanque, X. Wallart, and J. Grahn" Planar InAs/AlSb HEMTs With Ion-Implanted Isolation " IEEE Electron Device Lett. 33, 510 (2012)

25. W, Kowalsky, A. Schlachetzki, H. Wehmann, "Transferred-electron domains in $Ga_{0.47}In_{0.53}As$ dependence on the *nl* product," *Solid-State Electron*, vol. 27, no. 2, pp. 187-189, Feb. 1984.

26. Macpherson, R F, Dunn, G M, Pilgrim N J, Simulation of Gallium Nitride Gunn Diodes at various doping levels and temperatures for frequencies up to 300 GHz by Monte Carlo simulation, and incorporating the effects of thermal heating, Semicond. Sci. Technol. 23 (2008) 055005.

27. Dunn, G M, Rees, G J, David, J P R, Plimmery, S A, Herbertz, D C, *Monte Carlo simulation of impact ionization and current multiplication in short GaAs p+in+ diodes*, Semicond. Sci. Technol., vol. **12**, no. 1, pp. 111–120, Jan. 1997.

28. C. Li, "Design and characterisation of millimeter-wave planar Gunn diodes and integrated circuits," PhD thesis, 2012

29. Pilgrim, N J, Khalid, A, Dunn, G M, Cumming, D R S, Gunn oscillators in planar heterostructures, Semiconductor Science and Technology 23, (2008), article 075013.

30. Li, C, Khalid, A, Caldwell, S H P, Pilgrim, N J, Holland, M C, Dunn, G M, Cumming, D R S, Enhancement of power and frequency in HEMT-like planar Gunn diodes by introducing extra delta-doping layers, Microwave and Optical Component Letters, Vol. 53, No.7, pp.1624-1626, July 2011.

31. M. Fischetti, "Carlo simulation of transport in technologically significant semiconductors of the diamond and zinc-blende structures- Part I. Homogeneous Transport" IEEE Transations on Electron Devices, Vol. 38, (1991), pp634-649.

32. R.S.Rao, "Microwave Engineering" PHI ISBN-978-81-203-4514-0.

33. H. Kroemer, "Theory of the Gunn Effect", Proc. IEEE, vol 42, (1964), p.1736.

Figure Captions:

Figure. 1 A schematic diagram of the layer structure of the $In_{0.53}Ga_{0.47}As$ device.

Figure 2. Shows the main features of the fabrication process used to realize a submicron gap for devices as wide as 120μm.

Figure 3. An SEM image of a completed 600 nm x 120 μm planar Gunn diode is shown. The inset shows a close-up of the gap L_{ac}.

Figure 4. Measured IV characteristics of a typical 600 nm × 120 μm $In_{0.53}Ga_{0.47}As$ planar Gunn diode using 500 μs pulsed bias. The measured IV characteristic of a 1.3μm long planar Gunn diode [18] is also plotted for comparison.

Figure 5.(a)A schematic diagram of the experimental set-up to measure rf spectrum of the planar Gunn diode. The range of the spectrum analyser was extended with the help of external mixer and diplexer. (b) Measured spectrum of a 600 nm × 120 μm planar Gunn diode at applied bias of 3.31 V. The inset shows the zoomed in spectra at the oscillation frequencyof 307.5GHz. The spectrum analyser measurements setting were as follows: VBW: 200 kHz, RBW: 300 kHz, Span: 31.5 MHz.

Fig. 6. Measured power versus applied bias for a 600 nm long planar Gunn diode. Inset illustrates the J-band (220-325 GHz) power measurement setup: a J-band GSG probe, a J-band-to-W-band waveguide taper, a power sensor with W-band waveguide input, and a power meter

Fig.7. Oscillation frequency versus L_{ac} for devices simulated and experimentally measured. The dotted line is for eye guide only.

Figures:

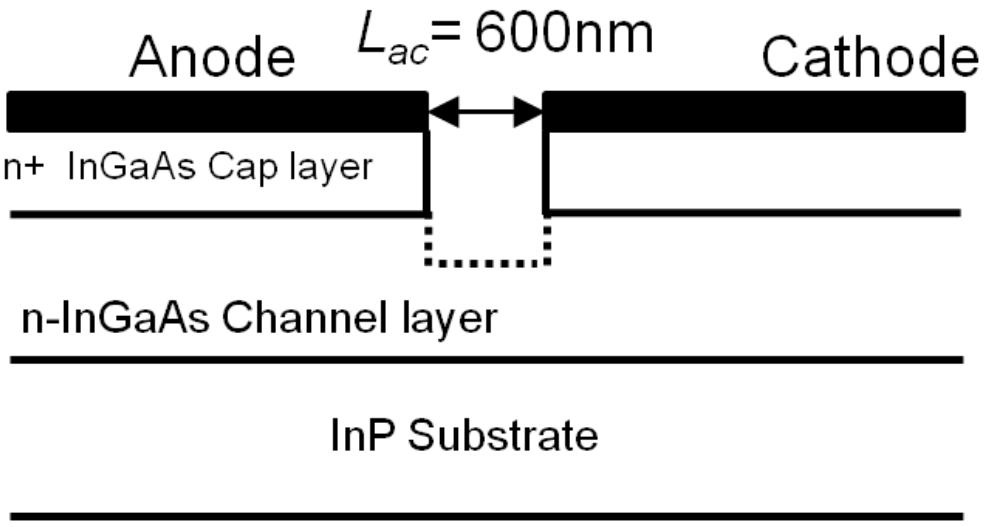

Figure. 1 A schematic diagram of the layer structure of the $In_{0.53}Ga_{0.47}As$ device.

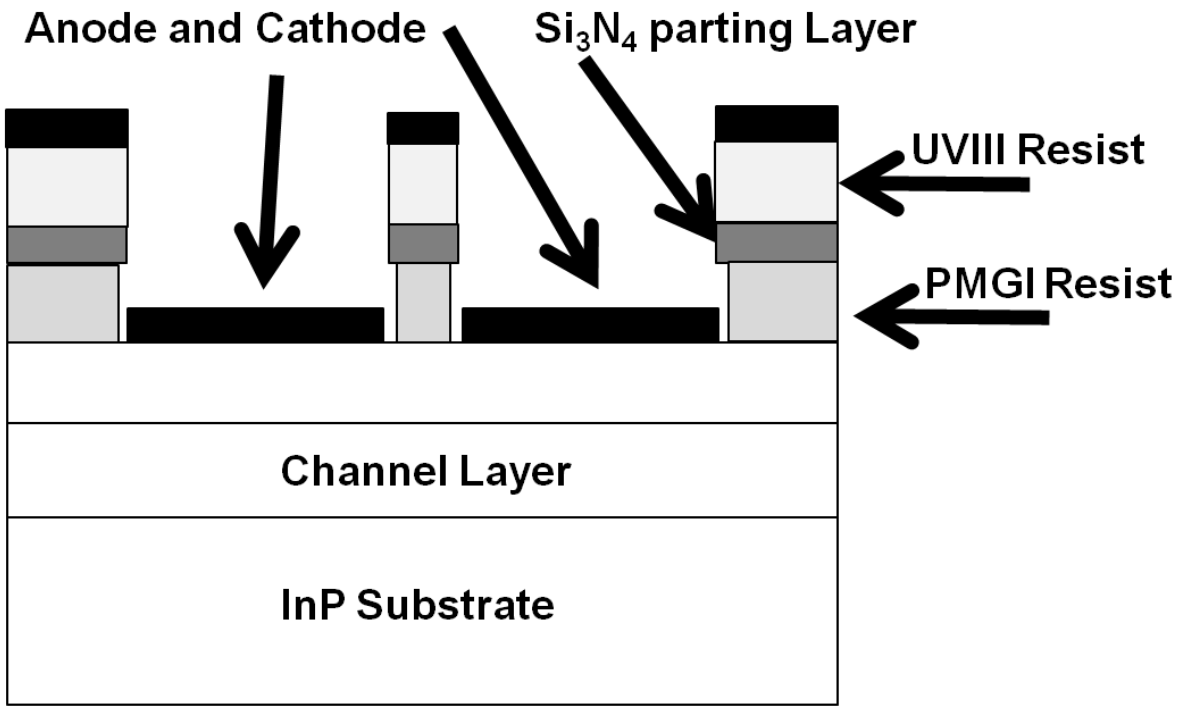

Figure 2. Shows the main features of the fabrication process used to realize a submicron gap for devices as wide as 120μm.

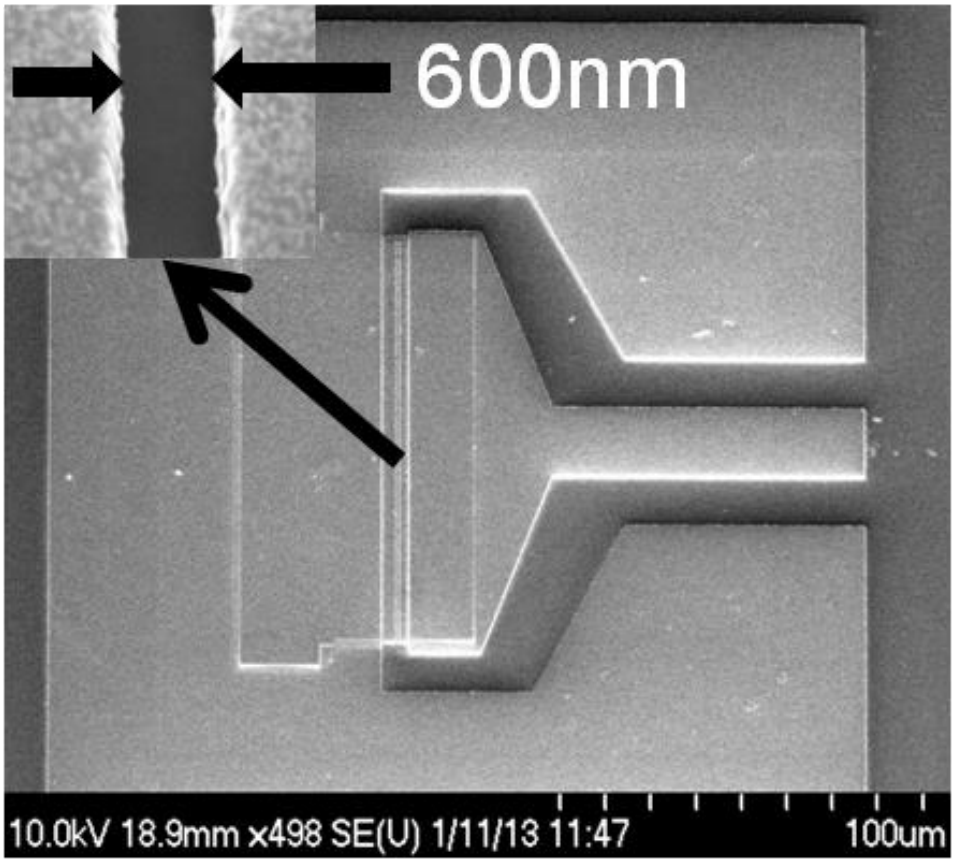

Figure 3. An SEM image of a completed 600 nm x 120 µm planar Gunn diode is shown. The inset shows a close-up of the gap L_{ac}.

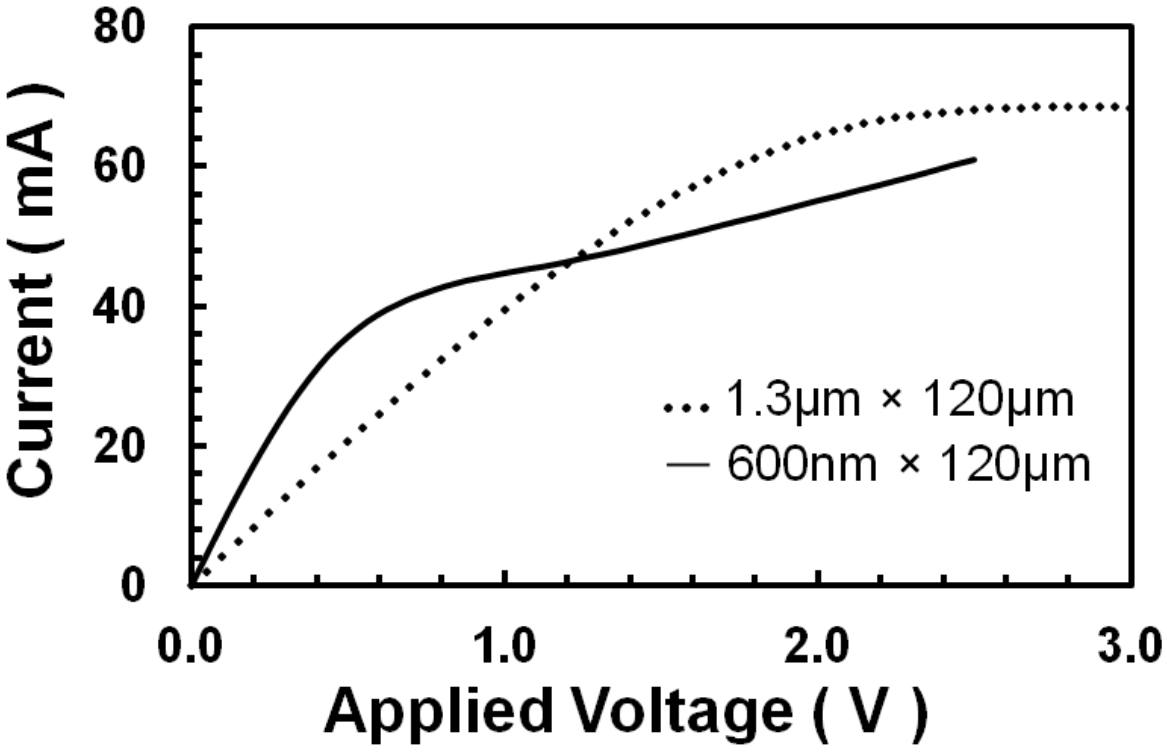

Figure 4. Measured IV characteristics of a typical 600 nm × 120 μm $In_{0.53}Ga_{0.47}As$ planar Gunn diode using 500 μs pulsed bias. The measured IV characteristics of a 1.3μm long planar Gunn diode [18] is also plotted for comparison.

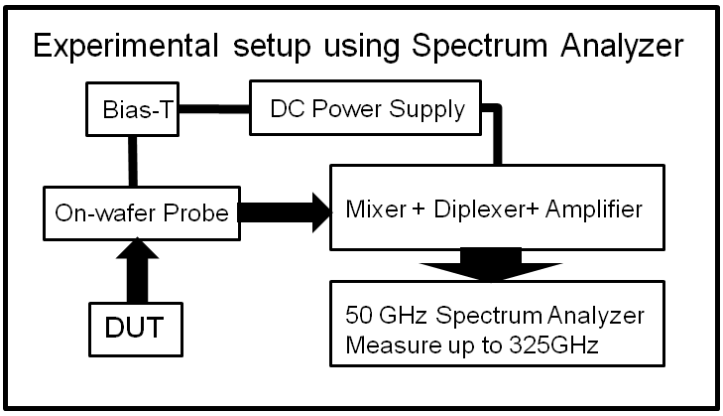

(a)

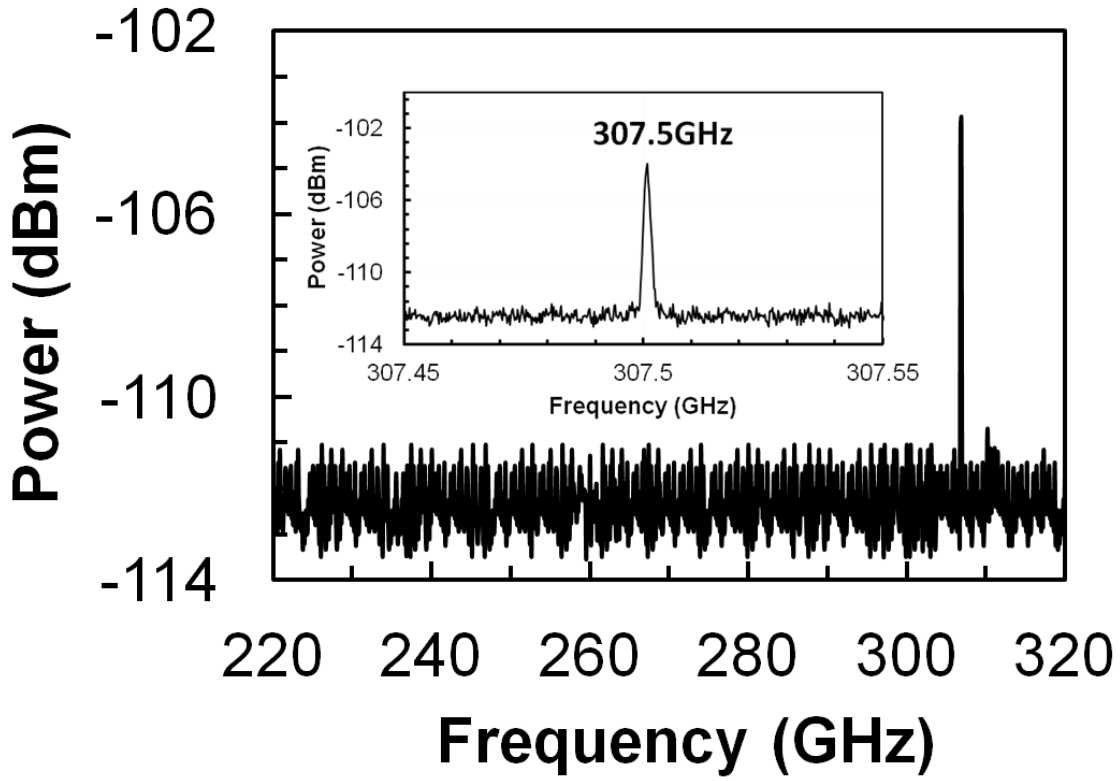

(b)

Figure 5. (a) A schematic diagram of the experimental set-up to measure the rf spectrum of the planar Gunn diode. The range of the spectrum analyser was extended using an external mixer and diplexer. (b) Measured spectrum of a 600 nm × 120 μm planar Gunn diode at applied bias of 3.31 V. The inset shows the zoomed in spectra at the oscillation

frequencyof 307.5GHz. The spectrum analyser measurements setting were as follows: VBW: 200 kHz, RBW: 300 kHz, Span: 31.5 MHz.

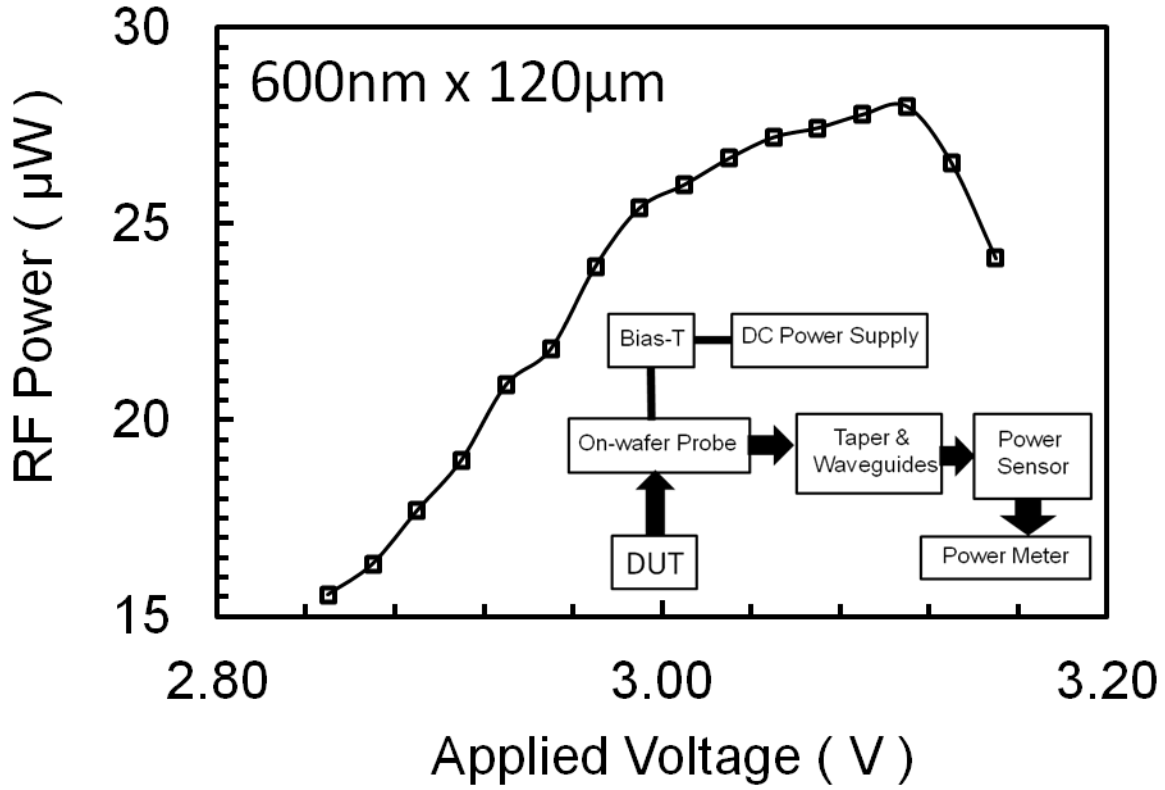

Fig. 6. Measured power versus applied bias for a 600nm long planar Gunn diode. Inset illustrates the J-band (220-325 GHz) power measurement setup: a J-band GSG probe, a J-band-to-W-band waveguide taper, a power sensor with W-band waveguide input, and a power meter

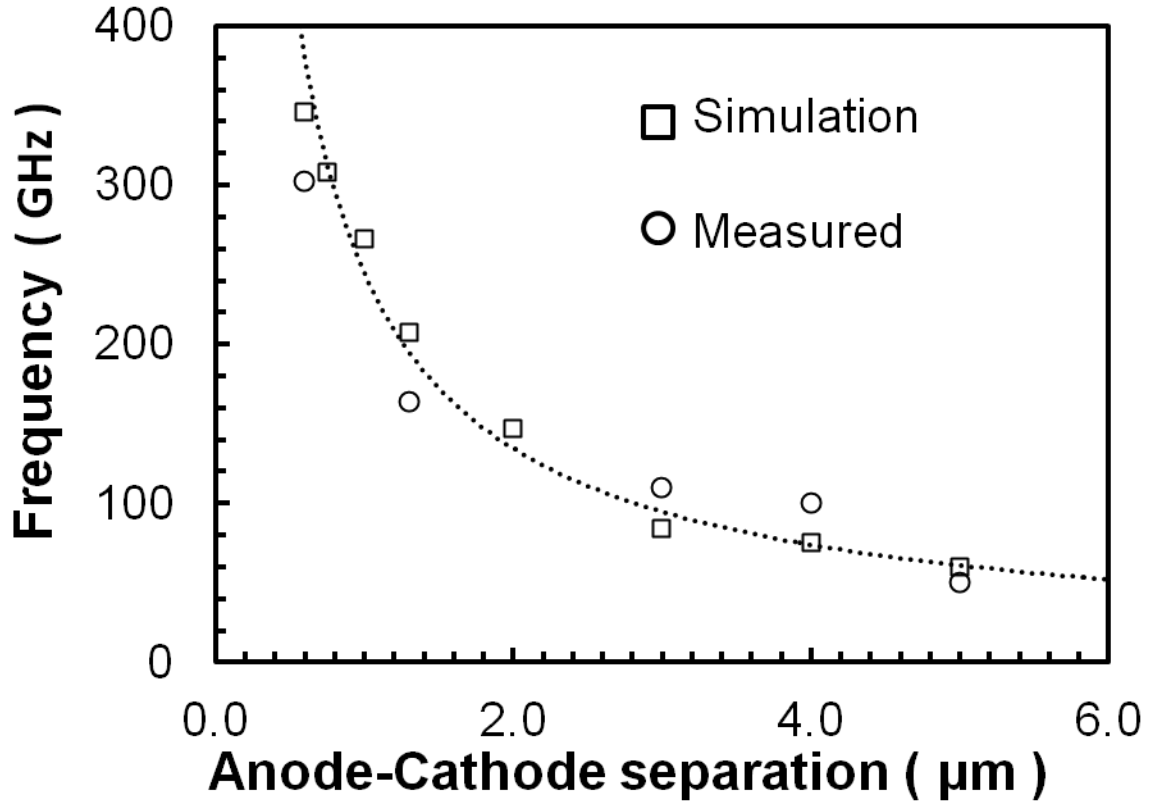

Fig.7. Oscillation frequency versus L_{ac} for devices simulated and experimentally measured. The dotted line is for eye guide only.